

# Origin of Giant Dielectric Response in Nonferroelectric $\text{CaCu}_3\text{Ti}_4\text{O}_{12}$ : Inhomogeneous Conduction Nature Probed by Atomic Force Microscopy

Desheng Fu,<sup>\*,†,‡</sup> Hiroki Taniguchi,<sup>‡</sup> Tomoyasu Taniyama,<sup>‡</sup> Mitsuru Itoh,<sup>‡</sup> and Shin-ya Koshihara<sup>†,§</sup>

*Exploratory Research for Advanced Technology (ERATO), Japan Science and Technology Agency (JST), 3-5 Sanbanchou, Chiyoda-ku, Tokyo 102-0075, Japan; Materials and Structures Laboratory, Tokyo Institute of Technology, 4259 Nagatsuta, Yokohama 226 8503, Japan; and Department of Chemistry and Materials Science, Tokyo Institute of Technology, Meguro, Tokyo 152-8551, Japan*

*Received April 18, 2007. Revised Manuscript Received November 22, 2007*

Local probing of conduction behaviors using atomic force microscopy clearly shows that the grain boundary of polycrystalline  $\text{CaCu}_3\text{Ti}_4\text{O}_{12}$  is semiconducting. In contrast, the grain is a mixture of semiconducting and insulating regions. This inhomogeneous conductive feature leads to giant dielectric response in  $\text{CaCu}_3\text{Ti}_4\text{O}_{12}$ . Theoretical analysis demonstrates that the dielectric response follows a typical Debye-type relaxation, and its unusual temperature dependence originates from the thermal activation behavior of free carries within the semiconducting regions in the grain. An effective way to control the electrical properties of CCTO is to control the defect density within a grain rather than the grain boundary.

## Introduction

The static dielectric constant of a material plays a decisive role in the miniaturization of capacitor-based devices. Since the dielectric constant is determined by the polarizability of a material, high dielectric response can be observed in polar materials, such as ferroelectrics or relaxor, due to the permanent polarization arising from the atomic displacement. Although relative dielectric constants over  $10^4$  may be found in ferroelectric or relaxor materials, it is limited within a narrow temperature range close to the phase transition. However, these temperature-sensitive high dielectric responses are undesirable for the practical applications of capacitor-based devices. Searching new materials with a temperature-independent dielectric constant larger than the exiting record is therefore a strong demand for practical applications.

Recently, several nonferroelectric materials have been reported to show a giant dielectric response up to  $10^5$ .<sup>1–4</sup> In particular, reports on giant dielectric response in pure

perovskite-like  $\text{CaCu}_3\text{Ti}_4\text{O}_{12}$  (CCTO)<sup>1,5</sup> have attracted wide interests in the material community.<sup>5–13</sup> The dielectric response of these materials shows the following common features: (1) The dielectric constant at low frequencies is extremely large at room temperature and is less dependent on frequency. As frequency increases to a megahertz range, it follows a Debye-type relaxation and drops to small values for a gigahertz range. (2) The low frequency response of the dielectric constant is nearly independent of temperature for a wide temperature range; however, it decreases rapidly to the same order of magnitude as that observed in the gigahertz range at room temperature, accompanying a large peak of dielectric loss (1–10) at a particular temperature depending on the measurement frequency.

Fully understanding the nature of giant dielectric response in these materials is of significant importance from both the

\* Corresponding author: tel 0081-45-924-5626; fax 0081-45-924-5386; e-mail fu.d.aa@m.titech.ac.jp.

<sup>†</sup> Japan Science and Technology Agency.

<sup>‡</sup> Materials and Structures Laboratory, Tokyo Institute of Technology.

<sup>§</sup> Department of Chemistry and Materials Science, Tokyo Institute of Technology.

- (1) Subramanian, M. A.; Li, D.; Duan, N.; Reisner, B. A.; Sleight, A. W. *J. Solid State Chem.* **2000**, *151*, 323–325.
- (2) Wu, J.; Nan, C. W.; Lin, Y.; Deng, Y. *Phys. Rev. Lett.* **2002**, *89*, 217601.
- (3) Yu, J. D.; Paradis, P. F.; Ishikawa, T.; Yoda, S.; Saita, Y.; Itoh, M.; Kano, F. *Chem. Mater.* **2004**, *16*, 3973–3975.
- (4) Xu, J.; Itoh, M. *Chem. Mater.* **2005**, *17*, 1711–1716.

- (5) Homes, C. C.; Vogt, T.; Shapiro, S. M.; Wakimoto, S.; Ramirez, A. P. *Science* **2001**, *293*, 673–676.
- (6) Chung, S. Y.; Kim, I. D.; Kang, S. J. L. *Nat. Mater.* **2004**, *3*, 774–778.
- (7) Sinclair, D. C.; Adams, T. B.; Morrison, F. D.; West, A. R. *Appl. Phys. Lett.* **2002**, *80*, 2153–2155.
- (8) He, L.; Neaton, J. B.; Cohen, M. H.; Vanderbilt, D. *Phys. Rev. B* **2002**, *65*, 214112.
- (9) Li, J.; Subramanian, M. A.; Rosenfeld, H. D.; Jones, C. Y.; Toby, B. H.; Sleight, A. W. *Chem. Mater.* **2004**, *16*, 5223–5225.
- (10) Lunkenheimer, P.; Fichtl, R.; Ebbinghaus, S. G.; Loidl, A. *Phys. Rev. B* **2004**, *70*, 172102.
- (11) Kim, I. D.; Rothschild, A.; Hyodo, T.; Tuller, H. L. *Nano Lett.* **2006**, *6*, 193–198.
- (12) Adams, T. B.; Sinclair, D. C.; West, A. R. *Adv. Mater.* **2002**, *14*, 1312–1323.
- (13) Adams, T. B.; Sinclair, D. C.; West, A. R. *Phys. Rev. B* **2006**, *73*, 094124.

viewpoints of technical application and fundamental research. Although intensive investigations have been focusing on clarifying the origin of giant response of CCTO, the conclusion has not yet been reached. Several possible mechanisms, including (1) fluctuations of lattice-distortion-induced dipoles in nanosize domains,<sup>5</sup> (2) electrode polarization effects due to the different work functions of an electrode and a sample,<sup>10</sup> (3) internal barrier layer capacitor (IBLC) effects originating from the insulating grain boundaries surrounding semiconducting grains,<sup>7</sup> and (4) intragrain insulating barrier effects,<sup>9,13–15</sup> have been proposed. Precise structural analysis indicates that all atoms in CCTO are under compression, the perovskite framework is extremely rigid, and no structural transition occurs in this  $Im\bar{3}$  centrosymmetric structure within 35–1273 K.<sup>1,16</sup> First-principle calculation shows that the  $Im\bar{3}$  structure is stable and the static dielectric constant is  $\sim 40$ .<sup>8</sup> Therefore, the origin arising from lattice distortion may be ruled out. More recently, the impedance response of CCTO ceramics has been demonstrated to be independent of the work function of the metal electrode,<sup>13</sup> indicating that the electrode polarization effects are not dominant. At present, the IBLC model of Schottky barriers at the interface between insulating grain boundaries and semiconducting grains is widely used to interpret experimental results.<sup>6,11,12,17</sup> In order to characterize the barrier structure, scanning Kelvin microscopy has been used to map the local potential difference on the polished surface of CCTO ceramics.<sup>6,17</sup> However, it should be noted that the grain boundaries are not visualized directly for the polished surface, and hence it is disputable whether the observed potential drop can be attributed to the grain boundary. Moreover, the critical shortcoming of the grain boundary barrier model is that it cannot provide a reasonable explanation for single crystals without grain boundaries, leading to the proposal of different mechanisms for polycrystals and single crystals.<sup>18</sup> Consequently, the origin of giant dielectric response in CCTO is still puzzling, and this situation might be an obstacle for controlling the electrical properties for technical applications.

In this paper, we unambiguously identify the conduction path in CCTO by local current probing with atomic force microscopy (AFM). In combination with scanning electron microscopy (SEM), we demonstrate that the grain boundary is conductive and cannot be an insulating barrier layer for the IBLC model. Our results point out that the giant dielectric responses of polycrystal and single crystal share the same origin: electrically inhomogeneous nature of CCTO crystal. We also model the unusual temperature dependence of the dielectric response successfully. It is essential that the rapid drop in the dielectric constant at low temperatures is due to the freezing of carriers in a semiconducting region within the crystal.

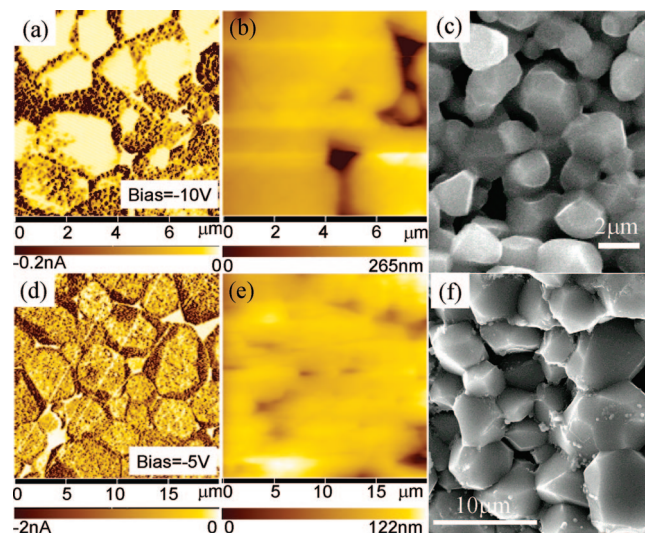


**Figure 1.** Current (a, d) and topographic (b, e) images obtained from polished surface of  $\text{CaCu}_3\text{Ti}_4\text{O}_{12}$  polycrystalline sample simultaneously. When comparing the current images to the corresponding SEM fracture images (c, f), it is clear that the grain boundary in  $\text{CaCu}_3\text{Ti}_4\text{O}_{12}$  is conductive. (a), (b), and (c) for sample A and (d), (e), and (f) for sample B with a further heat treatment at a higher temperature.

CCTO polycrystals were prepared by a solid-state reaction approach. Starting materials of  $\text{CaCO}_3$ ,  $\text{CuO}$ , and  $\text{TiO}_2$  were mixed and calcined at 1223 and 1273 K for 12 h each in an  $\text{O}_2$  atmosphere, with intermediate grindings to obtain a single-phased powder of CCTO. Dense ceramic rods were formed with a high hydraulic pressure of 300 MPa and sintered in  $\text{O}_2$  at 1323 K for 12 h. Sample A series were prepared directly from the sintered rod, while sample B series were prepared from the rod subjected to a further heat treatment in 2 atm  $\text{O}_2$  at a temperature close to the melting point by infrared radiation in an image furnace for several minutes. The heat treatment increases the grain size from  $\sim 2$  to  $\sim 10$   $\mu\text{m}$ . For electrical measurements, samples were polished and coated with Au by sputtering. Dielectric response to temperature (2–300 K) at 13 different frequencies between 100 Hz and 1 MHz and the frequency response (2 Hz–4.3 MHz) at room temperature were obtained by a commercially available LCR meter. In AFM measurements, we use the system of SII NanoTechnology Inc. (E-sweep Environment Control Unit controlled by SPI4000 Probe Station), which operates with a scanning-by-sample scheme and guarantees high accuracy of operation. One surface was coated with Au as a bottom electrode, and a conducting diamond-coated AFM tip was used as a top electrode to probe the current following underneath the tip toward the bottom electrode. During scanning, a bias voltage was applied between the AFM tip and bottom electrode, and the current and topographic images of polished surface were obtained simultaneously. After current imaging, AFM tip was then moved to the desired location to measure the local  $I$ – $V$  curves. Since the topography of the polished surface cannot offer information about the grain size and boundaries, SEM was used to reveal the fracture surface.

Figure 1 shows the AFM current, AFM topographic, and SEM fracture images for sample A (Figures 1a–c) and sample B (Figures 1d–f). For the current imaging, according

(14) Li, W.; Schwartz, R. W. *Appl. Phys. Lett.* **2006**, *89*, 242906.

(15) Chung, S. Y. *Appl. Phys. Lett.* **2005**, *87*, 052901.

(16) Moussa, S. M.; Kennedy, B. *J. Mater. Res. Bull.* **2001**, *36*, 2525–2529.

(17) Kalinin, S. V.; Shin, J.; Veith, G. M.; Baddorf, A. P.; Lobanov, M. V.; Runge, H.; Greenblatt, M. *Appl. Phys. Lett.* **2005**, *86*, 102902.

(18) Cohen, M. H.; Neaton, J. B.; He, L.; Vanderbilt, D. *J. Appl. Phys.* **2003**, *94*, 3299–3306.



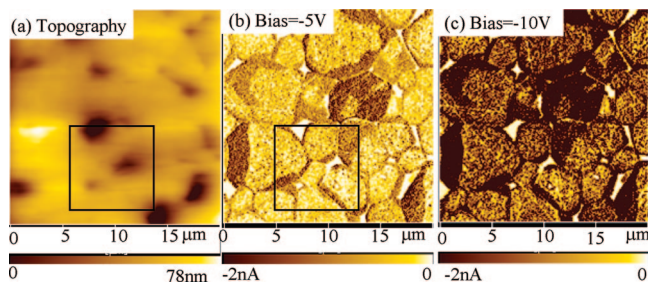


**Figure 2.** Current images mapping under different bias voltages for sample B in a different area: (a) topography, (b) bias voltage =  $-5$  V, and (c) bias voltage =  $-10$  V.

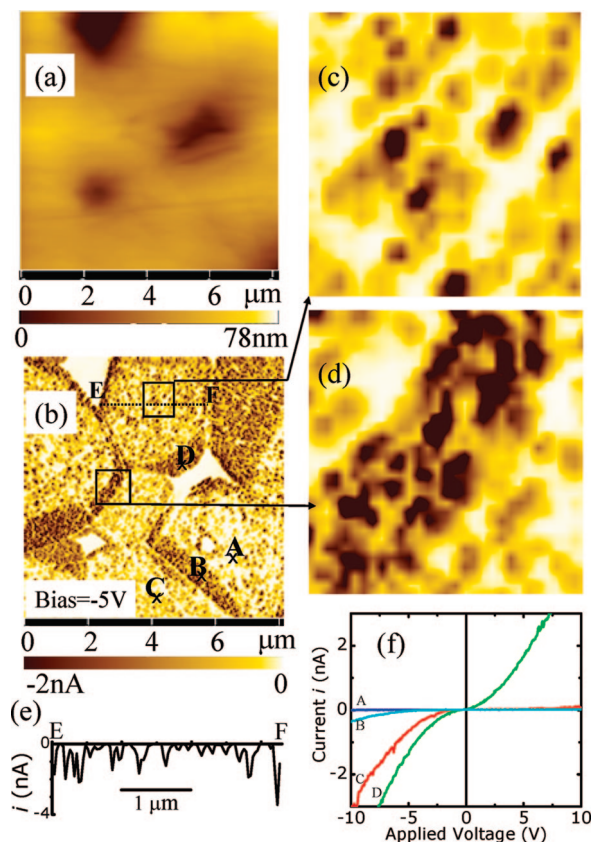


**Figure 3.** An expanded view of (a) the topography and (b) the current image for sample B for an area indicated in Figures 2a,b. (c) and (d) represent the zoomed-in current images in the grain center and grain boundary respectively. (e) Current profile along the line E–F across a grain. (f)  $I$ – $V$  curves observed at several typical locations. These figures show that a grain of  $\text{CaCu}_3\text{Ti}_4\text{O}_{12}$  consists of semiconducting and insulating regions.

to the  $I$ – $V$  characteristic curve (Figure 3f), a negative bias voltages between AFM tip and bottom electrode was used to prevent the block of current due to the interface barrier between AFM tip and sample surface. In these figures, the bright contrast represents an insulating state, while the dark contrast represents a conducting state. If the IBL model for semiconducting grains with insulating grain boundaries is correct, one can expect that a “bright” network of insulating grain boundaries blocks the “dark” conductive grains for samples with thickness less than the grain size, but if the sample thickness is greatly larger than the grain size, a blank current image will be observed because the current is completely blocked by the insulating grain boundaries. The thickness of our samples is  $\sim 150$   $\mu\text{m}$  and

greatly larger than the grain sizes ( $\sim 2$   $\mu\text{m}$  for sample A and  $\sim 10$   $\mu\text{m}$  for sample B), as indicated in the SEM images (Figures 1c,f); therefore, a blank current image is expected. Surprisingly, we observed a percolative conductive network with thickness of  $\sim 100$  nm, as shown in Figures 1a,d. We further observed the bias voltage dependence of current image for sample B in different regions, as shown in Figures 2b,c. It can be seen that the feature of current image is essentially independent of the bias voltage used in this studies, but current magnitude and dark region increase as increasing the mapping voltage, leading to the much dark contrast of the current image. A similar current pattern has been observed for all our CCTO samples, indicating that this conduction behavior is a common feature of CCTO.

Since the topography (Figures 1b,e) of the polished surface cannot provide any information about the grain boundaries, we cannot establish the origin of the conductive boundaries directly from the AFM measurements. However, when the current images (Figures 1a,d) are compared with the corresponding SEM images of fracture surface (Figures 1c,f), it can be seen immediately that the networks of conductive boundaries coincide quite well with those of grain boundaries. Consequently, we conclude that the grain boundaries are conducting. This conductive grain boundaries can be reasonably understood on the basis of possible  $\text{O}_2$  deficiency. For electron energy-loss spectroscopy (EELS) measurements of CCTO polycrystalline samples,<sup>19</sup> it was found that O/Ti ratio at the grain boundaries ranges from 2.90 to 2.65, indicating that 3–12% of  $\text{O}_2$  is deficient at the grain boundaries. It is well-known that  $\text{O}_2$  deficiency can easily give rise to a semiconducting or conducting state in titanate perovskites such as  $\text{SrTiO}_3$ ,<sup>20</sup>  $\text{CaTiO}_3$ ,<sup>21</sup> or  $\text{BaTiO}_3$ .<sup>22</sup> A possible  $\text{O}_2$  deficiency at the grain boundaries of CCTO polycrystalline sample should lead to a conductive behavior. Therefore, the conductive grain boundaries demonstrated here cannot be compatible with an insulating barrier involved in the conventional IBL model.

The question of whether there is a barrier structure within a grain now arises. In CCTO, the existence of a percolative conductive network, which is originated from the grain boundaries and formed in the bulk of the sample, allows us observe the conduction behaviors within grains for samples with thickness larger than grain size as those of samples with a single grain or single crystal. Here, we show that the electrically inhomogeneous structure consisting of semiconducting and insulating regions is indeed present within CCTO grains and provides the main source of barriers between conductive and insulating regions. This electrical inhomogeneity is visualized more clearly for sample B, which was subjected to a heat treatment at a higher temperature. Figures 3a,b show an expanded view of the topography and current image of sample B for an area indicated in Figures 2a,b. The zoomed-in current images in the grain center (Figure

(19) Wu, L.; Zhu, Y.; Park, S.; Shapiro, S.; Shirane, G. *Phys. Rev. B* **2005**, *71*, 014118.

(20) Schooley, J. F.; Hosler, W. R.; Ambler, E. A.; Becker, J. H.; Cohen, M. L.; Koonce, C. S. *Phys. Rev. Lett.* **1965**, *14*, 305–307.

(21) Kim, I.; Itoh, M.; Nakamura, T. *J. Solid State Chem.* **1992**, *59*, 77–86.

(22) Ikegami, S.; Ueda, J. *J. Phys. Soc. Jpn.* **1964**, *19*, 159–166.

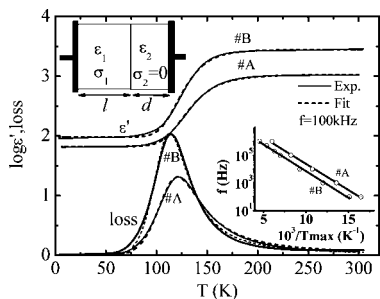


**Figure 4.** Temperature dependence of the dielectric constant and the loss of  $\text{CaCu}_3\text{Ti}_4\text{O}_{12}$ . The right inset represents the thermal activation behavior of the dielectric response. Dashed lines represent the simulation results using a simple model given in the left inset, which describe the electrically inhomogeneous structure within a CCTO grain.

**Table 1. Parameters Used To Simulate the Temperature Dependence of Dielectric Constant in CCTO Polycrystals**

sample	$\epsilon_1/a$	$\epsilon_1/a \delta$	$\tau_0$ (ns)	$E_0$ (meV)
A	67	1008	15.5	60.4
B	96	2716	7.0	67.7

3c) and current profile (Figure 3e) cross a grain indicated by a dashed line in Figure 3b, which clearly show the coexistence of conductive and insulating regions within the grain. The typical  $I$ – $V$  characteristics shown in Figure 3f indicates that the conductive regions is essentially semiconducting. The semiconducting nature within grains is likely due to defects of Ti on the Cu site or O defects. According to the structural analysis from neutron and synchrotron X-ray diffraction, defects of Ti on the Cu site occur in the rigid CCTO-type structure.<sup>9</sup> The Ti on Cu sites may indirectly provide charge carriers for the Ti 3d band and form the conducting regions accordingly. The defects of Ti on Cu sites were also confirmed by transmission electron microscopy<sup>19</sup> where a high density of planar defects associated with the movement of Ti to the Ca/Cu site was observed for the CCTO crystal. In addition to these planar defects, oxygen defects are also plausible. The fact that a high cooling rate during sample preparation greatly enhances the dielectric constant of polycrystalline samples<sup>23</sup> can be considered to be closely related to the  $\text{O}_2$  deficiency within the grain. Our local current measurements, in brief, demonstrate that CCTO has an electrically inhomogeneous nature that leads to a giant dielectric response in both single crystal and polycrystal.

On the basis of the results mentioned above, a simple double-layer model,<sup>24,25</sup> shown in the left inset of Figure 4, can be used to describe the heterostructural texture of conduction in CCTO consisting of a conductive layer with a thickness of  $l$ , a dielectric constant of  $\epsilon_1$  and a conductivity of  $\sigma_1$ , and an insulating layer with a thickness of  $d$ , a dielectric constant of  $\epsilon_2$ , and a conductivity of  $\sigma_2$ . The complex dielectric constant of this structure is then expressed as

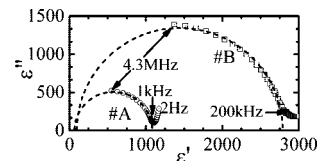


**Figure 5.** Cole-Cole plot for frequencies up to 4.3 MHz. The semicircle indicates a Debye-type relaxation with a characteristic frequency in the megahertz range at room temperature for CCTO. The high-frequency intersecting point gives the value of intrinsic dielectric constant of CCTO.

$$\epsilon^* = \frac{L}{l/(\epsilon_1 - i\sigma_1/\omega) + d/(\epsilon_2 - i\sigma_2/\omega)} = \frac{\epsilon_1}{a} + \frac{\epsilon_2}{a\delta} \frac{1}{1 + i\omega\tau} \quad (1)$$

where  $L = l + d$ ,  $a = 1 + \delta\epsilon_1/\epsilon_2$ ,  $\tau = \epsilon_2 a / \delta \sigma_1$ , and  $\delta = d/L$  represents the volume fraction of the insulating regions. Given that  $\epsilon_1 = \epsilon_2 \approx 100^{10}$  and the volume fraction of the insulating regions is very small ( $\delta \sim 0.001$ ), a giant value of the static dielectric constant  $\epsilon$  ( $\omega = 0$ )  $\sim 10^5$  can be estimated. This explains the reason for the giant dielectric constant of CCTO, which is dominated by the volume fraction of the insulating regions. Equation 1 also explains the Debye-type relaxation observed in CCTO. It is obvious that the relaxation is closely associated with the conductivity of the conductive layer.

Finally, we show that eq 1 can also be used to model the unusual temperature dependence of the giant dielectric response. From impedance measurements, it has been well established that the conduction of CCTO follows the Arrhenius form with activation energy of  $E_0$ <sup>7</sup>

$$\sigma_1 = \sigma_{10} \exp(-E_0/k_B T) \quad (2)$$

Using eqs 1 and 2, we obtain

$$\epsilon^* = \frac{\epsilon_1}{a} + \frac{\epsilon_2}{a\delta} \frac{1}{1 + i\omega\tau_0 e^{E_0/k_B T}} \quad (3)$$

where  $\tau_0 = \epsilon_2 a / \delta \sigma_{10}$ . From Figure 4, it is clearly seen that the experimentally obtained temperature dependence of the dielectric response of CCTO can be excellently reproduced by eq 3 with the parameters listed in Table 1. Using these parameters, we can also reproduce the frequency dependence of the dielectric constant obtained at room temperature very well (Figure 5). Since the volume fraction of insulating regions is extremely small in CCTO,  $\epsilon_1/a \cong \epsilon_1$ , the intrinsic static dielectric constant of CCTO with perfect atomic arrangement is then evaluated to be the order of  $\sim 100$ . This evaluation is in good agreement with the results obtained from infrared spectra (75–115),<sup>5</sup> gigahertz-range impedance analyzer techniques ( $\sim 100$ ),<sup>10</sup> and theoretical calculation ( $\sim 40$ ).<sup>8</sup> In fact, this value can also be obtained from low-temperature dielectric measurements directly. At low temperatures, because of the freezing of free carries, the dielectric response is contributed mainly by the lattice vibration. Our theoretical analysis indicates that the carrier within the semiconducting region has a barrier height of  $\sim 100$  meV (Table 1) to overcome. As temperature decreases and the carrier cannot get energy thermally higher than this barrier height, it should be frozen, consequently leading to two remarkable features in dielectric responses: (1) a rapid drop in dielectric constant and (2) a large dielectric dissipation

(23) Bueno, P. R.; Ramirez, M. R.; Varela, J. A.; Longo, E. *Appl. Phys. Lett.* **2006**, 89, 191117.

(24) Maxwell, J. C. *Electricity and Magnetism*; Oxford University Press: Oxford, England, 1873; Vol. I, Sect. 328.

(25) Wagner, K. W. *Ann. Phys. (Leipzig)* **1913**, 40, 53.

peak. Using the later feature, the barrier height can also be evaluated directly from the relationship between dissipation peak temperature and measurement frequency (the right inset of Figure 4). Now, it is clear that the rapid drop in the dielectric response at low temperatures is essentially due to the freezing of free carriers within the semiconducting regions in CCTO crystal.

In addition, theoretical analysis indicates that the carrier has a maximum response time of  $\sim 10$  ns (see Table 1). Since the carrier effect can be completely suppressed for time domain shorter than this response time, a high-frequency measurement technique, such as gigahertz-range impedance analyzer or infrared spectroscopy, should evaluate the intrinsic dielectric constant of CCTO even at room temperature, where the free carriers have a great influence on the dielectric response. Although the highest frequency of our dielectric measurements is  $\sim 4$  MHz, we can still extrapolate the data to high frequencies to get the intrinsic dielectric constant of room temperature (Cole–Cole plot shown in Figure 5). The estimated intrinsic value is close to the low-temperature dielectric constant. These results indicate that the static dielectric constant of CCTO crystal likely remains at the same constant for a wide temperature range, being consistent with the fact that the centrosymmetric structure of CCTO is extremely stable for wide temperature range of 35–1273 K.

It is worth pointing out that, since the electric response in CCTO is predominated by the electrical inhomogeneity of crystal, a direct way to tune the electric properties is to control the defect density within a grain. In our studies, we find that sample A, which has smaller grain size than sample B, shows a smaller value of dielectric constant ( $\epsilon \sim 1000$  in

frequency range of 1–100 kHz) at room temperature, indicating that some relationship between the grain size and dielectric response may exist in CCTO. Indeed, ref 12 shows that the dielectric constant at 10 kHz was greatly enhanced from  $\sim 9000$  for ceramics sintered for 3 h to  $\sim 280\,000$  for ceramics sintered for 24 h, while the grain size increases from  $\sim 10$  to  $\sim 300$   $\mu\text{m}$ , estimated from the given SEM images. Corresponding to the size dependence of dielectric response, the AFM measurements show that the density of current path within the small grain (sample A) is less than that of large grain (sample B), indicating that larger grain tends to have larger density of defect for CCTO. This inference is also supported by the TEM measurements of ref 19, in which higher density of the dislocations and planar defects was found in single crystal grown by the traveling-solvent floating-zone method as compared with polycrystals with grain size ranged from submicrons to tens of microns. For CCTO, controlling the grain size may be an effective way to tune the electrical properties of material.

In summary, we have established the nature of dielectric response in CCTO. The giant dielectric response is essentially due to the inhomogeneous conduction within the crystal, and the great drop at low temperatures is just the manifestation of freezing of free carriers. The present approach might be extended to systems showing similar features. Our results also point out that an effective way to control the electrical properties of CCTO is to control the defect density within a grain rather than the grain boundary, and CCTO is a proper material for sensor applications<sup>11</sup> rather than capacitor applications.

CM0710507